# Electronic structure of Cu-O chains in the high-$T_c$ superconductor $YBa_2Cu_3O_7$

H. Chen and J. Callaway
*Department of Physics, Louisiana State University, Baton Rouge, Louisiana 70803*

P. K. Misra
*Department of Physics, University of Rhode Island, Kingston, Rhode Island 02881*
(Received 11 December 1987; revised manuscript received 1 April 1988)

The electronic structure of Cu-O chains in the high-$T_c$ superconductor $YBa_2Cu_3O_7$ is investigated by self-consistent, all-electron, spin-polarized cluster calculations in the local-spin-density approximation for the cluster $Ba_4Cu_2O_7$. Four different charge states are considered. No localized moments are present on the Cu atoms in any of the charge states considered. The ground state of the cluster shows strong covalent bonding between the copper and oxygen atoms. Transition-state calculations are made to determine electronic relaxation occurring in photoemission, to calculate the effective Hubbard interaction parameter $U$ for both copper and oxygen sites, and to find the energy required for charge transfer between oxygen and copper atoms. The results are compared with experiment.

## I. INTRODUCTION

The superconductor $YBa_2Cu_3O_7$, which has a transition temperature above 90 K, is distinguished structurally from $La_2CuO_4$ (which, when some of the La is replaced by divalent Ba or Sr, gives a superconductor with $T_c$ close to 40 K) by the presence of linear Cu-O chains. Additional evidence indicates that if the chains are disrupted by removal of oxygen, the transition temperature decreases and superconductivity ultimately disappears.[1] For these reasons, much attention has focused on the Cu-O chains, although in the absence of a comprehensive theory of superconductivity in copper perovskites, the precise role of the chains and their importance relative to the distorted Cu(2)-O(2)-O(3) planes remains unclear.

Although several band calculations have not been reported for $YBa_2Cu_3O_7$,[2-8] we chose to investigate the electronic structure of this material by means of cluster calculations. It is, at the present time, difficult to make cluster calculations accurately for large systems; in fact, we have had to restrict our consideration to a portion of the material, rather than to consider a cluster big enough to represent the entire formula unit. Furthermore, it is also very difficult to simulate the effect of the crystalline environment on a cluster of atoms adequately. However, there are some offsetting advantages to cluster calculations which make this approach to electronic structure interesting and informative in the present case. These calculations, although restricted to a small number of atoms, can be made accurately self-consistent. Perhaps more significantly, it is possible to compute the energies of localized excitations with allowance for electronic relaxation through applications of Slater's transition-state approach.[9] This method is employed here to determine energies of peaks in the photoemission spectra, to compute the Hubbard electron interaction parameter $U$, and to find the energies of Cu—O charge-transfer processes. These results may be useful in estimating the parameters of model Hamiltonians, and in assessing theories of the interaction leading to superconductivity.

A problem which has received much attention in regard to the electronic structure of $YBa_2Cu_3O_7$ is the question of the valence of the copper atoms. If an elementary ionic model is adopted, a nonintegral value of 2.3 is obtained, suggesting that two of the Cu atoms should be in the $Cu^{2+}$ state, and one, in the $Cu^{3+}$ state. There are, in fact, two crystallographically inequivalent Cu sites in the unit cell: a single Cu(1) site associated with the Cu-O chains and two Cu(2) sites associated with planes. It has been argued from x-ray absorption measurements that the copper is divalent.[10,11] The possible existence of $Cu^{3+}$ is controversial.[10,12]

A closely related question concerns the question of magnetic moments on the copper atoms. In a localized picture, a $Cu^{2+}$ ion would be expected to have a $S=\frac{1}{2}$ and a moment. Measurements of the magnetic susceptibility of $YBa_2Cu_3O_7$ show an essentially temperature-independent magnetic susceptibility above $T_c$, in contrast to the Curie law behavior observed when Y is replaced by any one of several rare-earth ions.[13] The magnitude of the paramagnetic susceptibility is larger by a factor of (roughly) 2 than that predicted from the band-structure result for the density of states, indicating some Stoner enhancement. A possibility that $YBa_2Cu_3O_7$ might be a Kondo system with high $T_K$ is hard to exclude, but is open to the objection that the system fails to screen moments when Y is replaced by a rare-earth ion.[13] Nuclear quadrupole resonance measurements show no sign of localized moments.[14] One paramagnetic resonance experiment showed that at least some Cu ions are in the $Cu^{2+}$ state and have moments.[15] Another group failed to find either paramagnetic resonance or nuclear magnetic resonance signals.[16] The resolution of this problem is not clear.

Structurally, a unit cell of $YBa_2Cu_3O_7$ appears to contain three loosely coupled Cu-O subsystems: portions of two Cu(2)-O(2)-(3) planes and one Cu(1)-O(1)-O(4) chain. This calculation focuses on the latter, with which we include some of the neighboring barium atoms.

 

Specifically, the cluster considered is $Ba_4Cu_2O_7$. This cluster is shown in Fig. 1. The atomic positions in this cluster are determined from the structural information given by Beno *et al.*[17] Insofar as the picture of loosely coupled subsystems is valid, the cluster approach and the study of excitations localized on the cluster are reasonable.

Note that in an ionic model the $Ba_4Cu_2O_7$ cluster would be expected to be electrically neutral if the copper were in the $Cu^{3+}$ state, whereas if the copper were $Cu^{2+}$, the cluster would be expected to be negatively charged: $(Ba_4Cu_2O_7)^{2-}$. Calculations for these clusters convinced us that an ionic model was not appropriate; we have considered the charge states $(Ba_4Cu_2O_7)^{+}$ and $(Ba_4Cu_2O_7)^{2+}$ as well. In this way, we include the possibility that the cluster might serve as an electron donor to the rest of the crystal. In fact, we judge from the position of the Fermi level that $(Ba_4Cu_2O_7)^{+}$ is the most realistic. Our principal conclusions that the bonding is predominately covalent and no moments are present apply to all the charge states considered.

Photoemission studies, which are an important probe of the electronic structure have been reported by several groups.[10,18–21] An important discrepancy between these measurements and the results of band-structure calculations exists in that the energies of photoemission peaks indicate stronger electron binding than do the calculations, i.e., the peaks in the band-structure density of states are closer to the Fermi energy than are the experimental peaks by about 2 eV. This has been attributed to electronic relaxation in the final state.[22] We are able to confirm this suggestion by transition-state calculations. Additional transition-state calculations are made to estimate the Hubbard electron interaction parameter $U$, and the energies of charge-transfer transition between copper and oxygen. Our results are compared with experiment. A substantial degree of agreement is obtained. A preliminary account of this work has already been published.[23]

The procedures of our calculation are described in the next section, and the results are described in Sec. III. Our conclusions are summarized in Sec. IV.

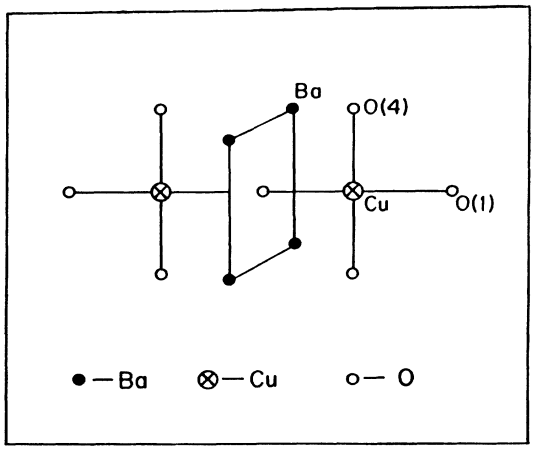


FIG. 1. Structure of the $Ba_4Cu_2O_7$ cluster, consisting of a $Cu_2O_7$ plane intersected by a $Ba_4$ plane perpendicularly in the middle.

## II. METHODOLOGY

The procedures of our calculation are discussed in this section. This work may be described succinctly as a self-consistent, all-electron calculation for a free cluster based on local-spin-density functional theory. Previous work by our group on the electronic structure of clusters has been restricted to clusters of cubic symmetry. Here, a new and more general program has been developed.

Local-spin-density functional theory yields a set of Schrödinger-like equations, (the Kohn-Sham equations) for a set of single-particle functions $\psi_i^\sigma(\mathbf{r})$ which are employed to construct the spin and charge densities. These equations are

$$[-\nabla^2+V^\sigma(\mathbf{r})]\psi_i^\sigma(\mathbf{r})=\epsilon_i^\sigma\psi_i^\sigma(\mathbf{r}), \tag{1}$$

where

$$V^\sigma(\mathbf{r})=2\sum_\sigma\int\frac{\rho^\sigma(\mathbf{r}')}{|\mathbf{r}-\mathbf{r}'|}d^3\mathbf{r}'+2\sum_\mu\frac{Z_\mu}{|\mathbf{r}-\mathbf{R}_\mu|}+V_{\rm ex}^\sigma(\mathbf{r}), \tag{2}$$

and

$$\rho^\sigma(\mathbf{r})=\sum_{j\ (\text{occupied})}|\psi_j^\sigma(\mathbf{r})|^2, \tag{3}$$

Atomic units are used throughout this paper (energies are sometimes expressed in eV when we think it is appropriate). We use the index $\sigma$ to denote the spins of electrons ($\uparrow$ or $\downarrow$). In Eq. (2), $R_\mu$ designates the position of the $\mu$th atom, and $Z_\mu$ is the corresponding atomic number. In Eq. (3), the index $j$ is summed over all occupied states in accord with the rules of Fermi-Dirac statistics. The quantity $V_{\rm ex}^\sigma(\mathbf{r})$ in Eq. (2) is a spin-dependent interaction term generally known as the exchange-correlation potential. In this paper, we take $V_{\rm ex}^\sigma(\mathbf{r})$ to have the von Barth–Hedin form with numerical parameters given by Rajagopal, Singhal, and Kimball.[24]

Equation (1) is usually solved by transforming it into a matrix equation. In the linear combination of Gaussian orbitals (LCGO) scheme, the single-particle wave functions are expanded into a set of Gaussian basis functions $u_j$,

$$\psi_i^\sigma=\sum_j C_{ji}^\sigma u_j. \tag{4}$$

Then, Eq. (1) is changed into a familiar secular equation,

$$\underline{H}^\sigma\underline{C}^\sigma=E^\sigma\underline{S}\underline{C}^\sigma, \tag{5}$$

where $\underline{S}$ is the overlap matrix ($S_{ij}=\langle u_i|u_j\rangle$) and $\underline{H}$ denotes the Hamiltonian matrix

$$H_{ij}^\sigma=\langle u_i|-\nabla^2+V^\sigma(\mathbf{r})|u_j\rangle. \tag{6}$$

To keep the size of this Hamiltonian at a manageable level, we used contracted basis sets: Ba($6s/4p/2d$); Cu($7s/5p/3d$); O($5s/2p/1d$). These sets were obtained from several sources.[25] In the case of copper, we used that given by Wachters[25] for the $^2D$ states, and we added to the Cu basis a polarization $p$ function with exponent of 0.155 and a diffuse $d$ function with exponent 0.1612. To study the question of basis set completeness, we have also

done some calculations using a slightly different basis set for Cu, where the most diffuse orbitals were removed and the basis set for the atomic states $^2S$ was used with a contraction scheme suggested by Bagayoko.[26] We did not find any appreciable changes in the final results by using this basis. The size of the Hamiltonian matrix we have to diagonalize is $319\times319$. The program does not require any specific choice of symmetry.

The most straightforward method of evaluating the matrix elements of the Coulomb interaction in Eq. (2) would require us to compute and store about $3\times10^8$ numbers. This is not practical for us at present. Therefore, we have made an auxiliary fit to the charge density to avoid this difficulty. We write

$$\rho^\sigma(\mathbf{r})=\sum_i a_i^\sigma f_i(\mathbf{r}) \tag{7}$$

to replace Eq. (3) in the evaluation of the Coulomb matrix elements. In Eq. (7), the $f_i(\mathbf{r})$ represent a set of basis functions composed of simple Gaussians of $s$ type ($e^{-ar^2}$) and $r^2$ type ($r^2e^{-ar^2}$) centered on each atom. The exponents of the $s$-type Gaussians are twice those of the corresponding functions used in the wave-function expansion, whereas those for the $r^2$-type Gaussians are twice those of the corresponding $p$-wave function. We also added a few diffuse basis functions in order to improve the quality of charge fitting in the bond region. The restrictions of the new fitting basis to spherical functions is a limitation of this approach which we are unable to assess quantitatively at this time. The fitting coefficients $\{a_i^\sigma\}$ of Eq. (7) are determined by a variational procedure which requires that the charge fitting should produce minimum errors in the electrostatic energy. This method was introduced originally by Sambe and Felton[27] and in its present form, by Mintmire and Dunlap.[28] It has been used by Lee *et al.* in the calculations for iron clusters.[29,30] The detailed formulation of this variational charge fitting procedure will not be given here. Interested readers should consult Refs. 29 and 30. The fitted charge density was found to be positive everywhere.

Another difficulty encountered in the evaluation of $H_{ij}$ arises from the fact that matrix elements of the exchange-correlation potential cannot be determined analytically. A separate fitting procedure is introduced for this potential, which is similar to Eq. (7):

$$V_{\rm ex}^\sigma(\mathbf{r})=\sum_j b_j^\sigma f_j(\mathbf{r}) , \tag{8}$$

where we have used the same set of fitting basis functions as in the case for charge fitting to reduce some extra work in the computation of the resulting three center overlap integrals. However, the fitting coefficients $\{b_j^\sigma\}$ of Eq. (8) are determined by a separate least-squares fitting procedure. We minimize the quantity,

$$D=\int d^3r\left[V_{\rm ex}^\sigma(\mathbf{r})-\sum_j b_j^\sigma f_j(\mathbf{r})\right]^2 . \tag{9}$$

One finds a set of linear equations to determine the $\{b_j^\sigma\}$. This set of equations can be written in matrix notation,

$$\underline{M}\cdot\underline{b}^\sigma=\underline{v}^\sigma , \tag{10}$$

with the definition of matrix $\underline{M}$,

$$M_{lm}=\int d^3r f_l(\mathbf{r})f_m(\mathbf{r}) , \tag{11}$$

and a vector $\underline{v}^\sigma$

$$v_k^\sigma=\int d^3r f_k(\mathbf{r})V_{\rm ex}^\sigma(\mathbf{r}) . \tag{12a}$$

It is important that the matrix elements $M_{lm}$ be obtained analytically so that Eq. (10) can be solved accurately. However, the elements $v_k^\sigma$ cannot be evaluated analytically. Numerical integration techniques are utilized here. We convert Eq. (12a) into a discrete summation over a set of sampling points $\{\mathbf{r}_i\}$ with corresponding weights $\{\omega_i\}$,

$$v_k^\sigma=\sum_i \omega_i f_k(\mathbf{r}_i)V_{\rm ex}^\sigma(\mathbf{r}_i) . \tag{12b}$$

The procedure of generating sampling points in Eq. (12b) follows the Diophatine method,[31] which was first applied in electronic structure calculations by Ellis *et al.*[32,33] Essentially, this set of points is generated by a random point technique with an equal-interval sampling in the angular coordinates $(\theta,\phi)$. The radial distribution of these points follows a single function

$$\mu(r)=\frac{1}{r^2(1+e^{\alpha(r-r_0)})} \tag{13}$$

around each atom.[34] In Eq. (13), $\alpha$ and $r_0$ are two parameters which can be adjusted to achieve optimal fitting (usually, $\alpha\sim1$, and $r_0\sim1$ in atomic units). The overlap integrals of Eq. (11) could also have been evaluated numerically using the sampling points just mentioned, as it might appear to be more consistent. We found that, however, direct analytical integration of Eq. (11) produced more accurate fitting of $V_{\rm ex}^\sigma$, especially in the regions close to the nucleus.

To check the quality of this choice of points, we used them to integrate numerically the total charge of the system, and we found the error was about 0.6%. We also compared the actual $V_{\rm ex}^\sigma$ with the fitted $V_{\rm ex}^\sigma$ in some regions of the cluster. We found that the error was less than 1% in the atomic core region and a few percent in the interstitial bond region. In view of the relative smallness and smoothness of the exchange-correlation potential in comparison with other terms in Eq. (2), we believe the current treatment of $V_{\rm ex}^\sigma$ is adequate and efficient.

The problem of simulating the effect of the crystal environment on a cluster which is intended to represent a portion of a solid (embedding) is difficult, and in our opinion, has not been solved satisfactorily at the present time. A procedure which has been employed in the case of ionic clusters is to place point charges (fractional if necessary) at the positions of the nearest shell of atoms omitted from the cluster.[35,36] In the present case, embedding potentials for the $Cu_2O_7$ system representing the chain are furnished by the four neighboring $Ba^{2+}$ ions. It appears from the results that the $Ba_4Cu_2O_7$ cluster is close to neutral (in regard to charge), so that it is not necessary to add additional charges. Insofar as the Cu(1)-O(1)-O(4) chains are somewhat isolated from each other and the remainder of the crystal, this procedure may be reasonably satisfactory.

The embedding problem would disappear if we performed a self-consistent band calculation. If only the electronic structure of the ground state of the crystal were of interest, the band-structure approach certainly would be preferable. It appears from the comparison of the present results with current band-structure calculation,[2-8] and with experiments as discussed in Sec. III that the electronic structure of the cluster ground state as obtained here is substantially consistent with the other studies mentioned. However, the principal reason for undertaking cluster calculation is not to study the ground state but rather to investigate localized excitations. Use of the transition-state method makes this simple for a small cluster, while it would be extremely difficult within the framework of a full band-structure calculation. Of course, the cluster calculations are meaningful only for those types of excitations which are localized within the cluster.

## III. RESULTS AND DISCUSSION

### A. Cluster ground state

As mentioned in the Introduction, we have studied the $Ba_4Cu_2O_7$ clusters in four different charge states since it was not clear at first what would be the charges of the oxygen and copper atoms. Table I lists the Fermi energy of the $Ba_4Cu_2O_7$ cluster in 2+, 1+, 0,2− charge states. Judging from the energy of the Fermi level, we think that $(Ba_4Cu_2O_7)^{1+}$ should represent the original crystal more realistically. On the other hand, we find that all four clusters give essentially the same results for the change distribution and energy-level structure.

The actual charge state of the cluster, in reference to a bulk sample, cannot be determined rigorously. If it were possible to isolate a portion of the real crystal corresponding to the cluster we study, we might expect to find in a time average that the charge state of the cluster was not an integer. Our calculation, however, is performed only for the limited number of states listed. Two plausible but inconclusive arguments suggest that the choice of 1+ is most reasonable: (1) Results of a large number of calculations we have performed for other clusters with transition-metal atoms for which the charge state is known in advance, including NiO,[36] yield a Fermi energy in the neighborhood of 4 eV below the vacuum level. A Fermi energy just at the vacuum level (our result for a neutral cluster) or 9 eV below (the 2+ state) seems to be unreasonable. (2) Energy-band calculations[2-8] unfortunately do not show the vacuum level, but find that the band associated with the Cu-O chains extends about 2 eV above $E_F$. If it is assumed that an electron could be put into one of these states without escaping from the crystal, the Fermi energy should be more than 2 eV below the vacuum level. We are unaware of any evidence for an exceptionally low work function. These arguments ignore possible electrostatic energy shifts due to charging and electrostatic potentials on the atoms surrounding the cluster [Y, and the Cu(2)-O(2)-O(3) planes]. The generally good comparison of the density of states with that obtained from band calculations argues against major errors in our work due to charging; but it would be necessary in order to make more conclusive statements to have band results in which the position of the Fermi level was specified with respect to the vacuum.

TABLE I. Fermi level of $Ba_4Cu_2O_7$ clusters.

| | $E_F$ (Ry) |
|---|---|
| $(Ba_4Cu_2O_7)^{2+}$ | −0.661 |
| $(Ba_4Cu_2O_7)^{+}$ | −0.321 |
| $Ba_4Cu_2O_7$ | −0.008 |
| $(Ba_4Cu_2O_7)^{2-}$ | 0.532 |

We want to emphasize that we did not find any local magnetic moments in the $Ba_4Cu_2O_7$ clusters in any of the four different charge states even though our calculations are spin polarized. The calculations were begun with the assumption that there is a moment, but the input moment disappeared quickly during the first few iterations leading to self-consistency. Other cluster ground-state properties obtained here such as high covalency of O-$p$ bond, strong hybridization between Cu $d$ and O $p$ orbitals, and low valency of the copper atom all support this zero moment result in a consistent way.

Local-spin-density functional theory as implemented for clusters with presently available exchange-correlation potentials seem to err in the direction of predicting local moments in systems where they do not exist (dilute Ni in Cu, for example[37]). Therefore, the failure to find a moment in these calculations is an indication that no moment is to be expected.

In contrast, antiferromagnetic order has been observed in $La_2CuO_{4-y}$, with small moments and a Néel temperature of 220 K.[38] However, in the $La_2CuO_4$ system, every copper atom is inside an elongated octahedron with six oxygen atoms at each corner. In this geometry, which is rather different from that studied here, a local moment can be formed as demonstrated by the antiferromagnetism of NiO. However, we are not aware that local-density band (or cluster) calculations have obtained covered moments in $La_2CuO_4$. The rather small value of the Hubbard $U$ obtained in local-density calculations for NiO suggests that such calculations may overestimate $p$-$d$ hybridization and thus underestimate localization (and magnetism) in transition-metal–oxygen systems. It seems clear now that no Cu atoms have static moments above $T_c$ in $YBa_2Cu_3O_7$. But recent work shows that if the oxygen content of $YBa_2Cu_3O_7$ is reduced to about $O_6$, which destroys the Cu-O(1)-O(4) chains, a moment and antiferromagnetic order can be observed.[39]

The prediction of local-spin-density theory that there are no moments on copper contrasts with the results of more conventional quantum chemical calculations in which moments are obtained[40] for a variety of clusters, including the chains studied here. We believe that methods based on the Hartree-Fock approximation may err in the opposite direction from local density in overemphasizing a tendency toward localization.

The valence-electron populations of the atoms in the cluster are presented in Table II. Two methods have been

TABLE II. Valence population analysis for each atom.

| | Mulliken population | | | | | | Numerical integration | | | | |
|---|---|---|---|---|---|---|---|---|---|---|---|
| | Ba $s$ | Cu $s$ | Cu $p$ | Cu $d$ | O $s$ | O $p$ | Ba | Cu | O(1) center | O(1) edge | O(4) |
| $(Ba_4Cu_2O_7)^{2+}$ | 0.15 | 0.25 | 0.34 | 9.32 | 0.13 | 4.92 | 0.12 | 9.56 | 3.0 | 2.73 | 3.02 |
| $(Ba_4Cu_2O_7)^{+}$ | 0.22 | 0.24 | 0.32 | 9.30 | 0.12 | 5.05 | 0.13 | 9.57 | 3.0 | 2.85 | 2.99 |
| $Ba_4Cu_2O_7$ | 0.33 | 0.23 | 0.30 | 9.30 | 0.10 | 5.16 | 0.15 | 9.59 | 3.0 | 2.87 | 2.98 |
| $(Ba_3Cu_2O_7)^{2-}$ | 0.67 | 1.03 | 0.42 | 9.18 | 0.02 | 5.25 | 0.21 | 9.66 | 3.0 | 2.88 | 2.98 |

used to analyze the valence-electron charge distribution. One is the traditional Mulliken population analysis in terms of atomic states ($s$, $p$, $d$). The oxygen atoms are treated as equivalent in the Mulliken analysis given in Table III, although there are some differences between the three different oxygen sites in the cluster. For the $(Ba_4Cu_2O_7)^{+}$ cluster, this analysis yields the total $(s+p)$ charges for the oxygen atoms: 6.09, O(1) center; 4.54, O(1) edge; and 5.27, O(4). The Mulliken procedure is not always reliable quantitatively, particularly for diffuse functions. Therefore, we have considered another method which involves numerical integration of the charge density through a sphere around each atom. The sphere radii were chosen to be covalent radii (Ba: 2.47, Cu: 2.21, and O: 1.38, in a.u.). The results of these two analyses are in fairly good agreement, except for oxygen.

Several important conclusions can be drawn from Table II. We first note that present calculation clearly indicates that copper atom is in a low valence state. $Cu^{3+}$ is not found. Numerically, Cu is in a state around $Cu^{1.4+}$. This result is qualitatively consistent with the conclusions of Ref. 21. There it is observed that the oxidation of Cu in $YBa_2Cu_3O_7$ is less than that of CuO, and that $Cu^{3+}$ does not occur. In reality, the copper atom may fluctuate between $Cu^{+}$ and $Cu^{2+}$ states and produce instantaneous moments. But the study of fluctuation effects is beyond the scope of this work. Consistent with the observation that Cu atoms are in low valence states, we find the oxygen atoms are not in a strongly negatively charged state. Most of the oxygen is present as $O^{-}$. From this and from the density of states described below, we conclude that O $p$ holes are important in the conduction mechanism. Also note that no appreciable differences between the population of the center O(1) and the O(4) sites are found in the numerical calculation even though the copper atom beyond O(4) is omitted in the cluster. That the population of O(1) at the edges is always smaller can be attributed to the special geometry of the cluster studied here but contrasts with the result for O(4). Detailed studies of the charge distribution on an orbital-by-orbital basis indicate that the states near $E_F$ are oxygen $2p$ functions centered around the edge O(1) atoms. The relatively high energy of these states can be attributed to the omission of the copper atoms beyond. Therefore, the cluster calculation overestimates the O($2p$) content near the Fermi surface in comparison with band calculations.

TABLE III. Core levels (Ry) in $(Ba_4Cu_2O_7)^{+}$.

| | Ba | Cu | O |
|---|---|---|---|
| 1$s$ | −2608.2 | −641.87 | −37.24 |
| 2$s$ | −401.65 | −76.51 | −1.74 to −1.46 |
| 2$p$ | −379.34 | −67.24 | |
| 3$s$ | −84.84 | −8.32 | |
| 3$p$ | −75.26 | −5.49 to −5.36 | |
| 3$d$ | −57.29 | | |
| 4$s$ | −16.71 | | |
| 4$p$ | −13.25 | | |
| 4$d$ | −7.00 | | |
| 5$s$ | −2.60 to −2.50 | | |
| 5$p$ | −1.86 to −1.45 | | |

The fact that the value of the charge given by integration of the density around each copper atom is very close to that of the Cu $d$ Mulliken population analysis indicates Cu $d$ electrons are substantially localized inside a sphere of a radius about 2.21 a.u. On the other hand, the small results obtained by numerical integration around the oxygen sites indicate that the oxygen charge distribution is quite diffuse. The general picture of the copper-oxygen subsystem which emerges from these calculations, including the results presented in Table II, the absence of moments on the Cu atoms, and the more detailed Mulliken population analysis for the individual eigenstates (not shown here) emphasizes O$p$-Cu$d$ hybridization and covalent bonding. Finally, we note that each of the Ba ions simply donates its two valence electrons to the Cu-O chain.

Next, we study the distribution of single-particle eigenvalues in the ground state. Core levels for each atom are listed in Table III. Due to their diffuse nature, O 2$s$ states and Ba 5$p$ states are hybridized with each other producing a distribution with a width of about 5.5 eV. Experimental results[11,20] indicate Ba 5$p$ states span a range of about 5-6 eV but the binding energies for this status are lower than the results obtained from this cluster study. A similar discrepancy is also found for the Ba 5$s$ states, where the experimental value of binding energy is about 2.13 Ry while this work gives a value around 2.24 Ry. Although only a minimum basis is used for the Ba atoms here, so that the accuracy of the Ba levels is limited, these results may indicate that the charge state of Ba in the bulk material is slightly different from that found here. A discrepancy here is not unexpected since the Ba atoms are boundary atoms in this cluster.

X-ray spectra of Ref. 11 indicate the Cu 3$p$ state has a binding energy of 5.42 Ry; the Cu 2$p$ state, 69.0 Ry; and the O 1$s$ state, 38.9 Ry. These values are comparable to but lower than the single-particle energies listed here.

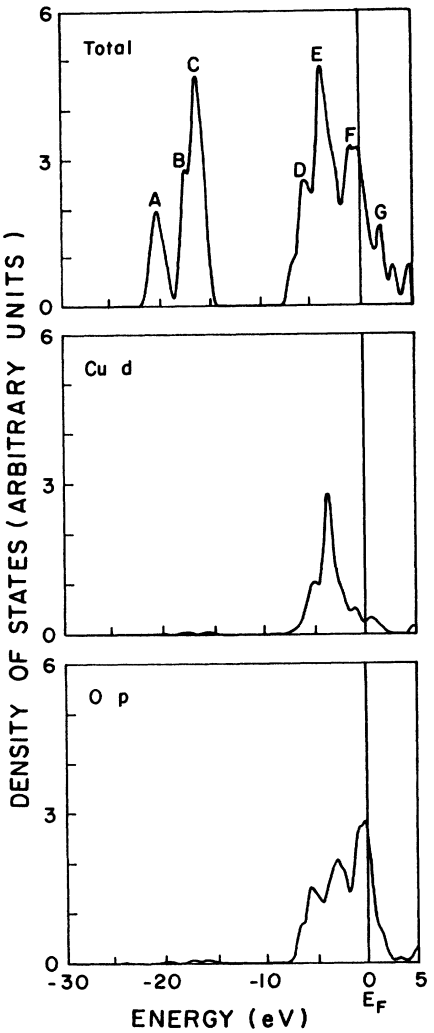


FIG. 2. Top: total electronic density of states. Middle: projected density of states for Cu *d*. Bottom: projected density of states for O *p*. The Fermi energy has been chosen as the zero of the energy scale.

Even though they are all lower than the cluster results, we notice that single-particle energies agree with experimental results better for the Cu 3*p* states than for the Cu 2*p* state. This is due to differing amounts of final-state relaxation. Transition-state calculations for these core states are reported in Sec. III B.

We present the valence-band single-particle levels graphically in Fig. 2, where each single-particle level has been broadened by a Gaussian function $e^{-(E-E_i)^2/\Delta^2}$ with $\Delta=0.5$ eV. Table IV lists the results of the Mulliken population analyses for a few energy levels centered around the major peaks of Fig. 2. It is quite obvious from this table and Fig. 2 that the valence band is mainly composed of Cu *d* and O *p* electrons. The valence-band width is about 11 eV which is a little wider than that obtained from band calculation[2-8] (about 7 eV). Very close to the Fermi energy, states are principally of O *p* type as discussed above. At about 2 eV above Fermi level, a peak of unoccupied Ba 6*s* states is found (peak *G*). At 0.8 eV below $E_F$, peak *F* is composed of states predominately O *p*. Another peak, *E*, with states predominately Cu *d* is found at about 3.4 eV below the Fermi level.

In general, the valence-band picture presented here is consistent with the results obtained from the energy-band calculations cited earlier.[2-8] As can be seen from Table IV, the state at the Fermi level is mainly of O *p* nature, while band calculations indicate more Cu *d* components than the present cluster results. But, the main results of this cluster calculation such as the strongly covalent bonding, nonexistence of magnetic moments, the location of peaks in density of states, as well as the chemical origin for each peak, agree fairly well with the results of most of the band calculations (especially with Ref. 4, where detailed comparison is possible). However, we also note here that one set of results for energy bands based on LMTO-ASA method[6] differs rather substantially from the results obtained by other band calculations. Judging from graphical data, the results of Ref. 6 seem to imply that Cu *d* states are concentrated at about 1-2 eV below the Fermi level.

### B. Transition-state results

In Ref. 23, our calculated density of states was compared with the ultraviolet resonant photoemission measurements of Kurtz *et al.*[19] A substantial degree of agreement was found there. However, as in the band calculations cited,[2-8] the calculated density of states is shifted to higher energy with respect to the peaks in photoemission spectrum by about 2 eV. We show here through transition-state calculations, that this shift is due to elec-

TABLE IV. Results of a Mulliken population analysis for a few selected single-particle levels. Labels for each peak are defined in Fig. 3.

| Location | Energy (eV) | Ba*s* | Ba*p* | Cu*s* | Cu*d* | O*s* | O*p* |
|---|---|---|---|---|---|---|---|
| Peak *A* | −24.2 | | 0.84 | | | 0.13 | |
| Peak *B* | −21.8 | | 0.30 | | | 0.59 | |
| Peak *C* | −20.4 | | 0.49 | | | 0.44 | |
| Peak *D* | −9.47 | | | | 0.44 | | 0.53 |
| Peak *E* | −7.75 | | | | 0.69 | | 0.28 |
| Peak *F* | −5.18 | | | | 0.11 | | 0.86 |
| $E_F$ | −4.37 | | | | 0.04 | | 0.94 |
| Peak *G* | −2.30 | 0.90 | | 0.04 | | | 0.06 |

tronic relaxation.

Details of Slater's transition-state calculation procedure have been described elsewhere.[9] As shown there, the transition-state procedure is expected to give an accurate evaluation of electronic transition energy because the dependence of total energies on occupation number is eliminated up to the third power. Thus, results obtained by transition-state procedure are expected to be different from those obtained from ground-state eigenvalues if particle interactions are not negligible. This is exactly the case for the $Ba_4Cu_2O_7$ cluster studied here. For a state in peak $F$ of Fig. 3, the ionization energy obtained from the transition-state procedure is 0.533 Ry while the value directly obtained from single-particle eigenvalues is 0.381 Ry. We thus see that peak $F$ should be shifted down toward lower energy by 0.152 Ry, about 2 eV, when electronic relaxation is taken into account. A similar transition state calculation on a state in peak $E$ gives an ionization potential of 0.739 Ry. We conclude from comparison with the eigenvalue listed in Table IV, that this peak should be shifted down by about 2.3 eV. Therefore, after inclusion of electronic relaxation, the locations of peak $E$ and peak $F$ of Fig. 2 should be at 5.7 and 3.0 eV below $E_F$. This is a substantial improvement over the single-particle picture in comparison with experiments where photoemission spectra show two peaks 4.6 and 2.6 eV below $E_F$ from Ref. 20, and 4.3 and 2.3 eV from Ref. 18. The physical processes likely to be involved in the electronic relation are discussed in Ref. 22.

Charge-transfer transition can also be studied via the transition-state procedure. However, in contrast to the results for the ionization potential, we find that values obtained from transition-state calculations are not significantly different from values deduced from single-particle eigenvalue differences. Through a transition-state procedure, we calculated the transition energy of an electron from a Cu $d$ state to the first unoccupied state (61% O $p$ from Mulliken analysis) to be about 4.4 eV, while directly from eigenvalues we found 4.2 eV. Since the bandwidth of predominately Cu $d$ states is about 1 eV (from Fig. 2), we infer that the charge-transfer energy from Cu $d$ to unoccupied O $p$ is in the range of 3.9–5.2 eV. The small difference between the results from transition-state calculation and those from eigenvalues implies that electronic relaxation effects are relatively small for this process as would be expected in a highly hybridized situation. Similar observations have been made about Ni $d$ to O $p$ transitions in a $NiO_6^{-10}$ calculation.[36]

We calculated the electron affinity energy for the unoccupied peak $G$ of Ba $6s$ state. The transition-state calculation gives a value of about 0.5 eV. The eigenvalue of the corresponding state is $-2.3$ eV. The charge-transfer energy from O $p$ to Ba $s$ can then be calculated from the difference between the O $p$ ionization potential (7.25 eV) and the Ba $6s$ affinity energy to be around 6.7 eV.

The Hubbard parameter $U_{dd}$ which measures the intra-atomic Coulomb interaction energy between $d$ electrons on Cu sites is of considerable importance because several model theories of high-temperature superconductivity are based upon nonphonon mechanisms[41] stressing the importance of electronic correlations as studied through the Hubbard Hamiltonian. When all $d$ orbitals are almost full in the single-particle picture, the Hubbard parameter can be estimated by the following procedure:

$$U_{dd}=\Delta E_1-\Delta E_2\,, \tag{14}$$

with

$$\Delta E_1=E_{\rm tot}(n_d^{\uparrow},n_d^{\downarrow})-E_{\rm tot}(n_d^{\uparrow}-1,n_d^{\downarrow})\,, \tag{15}$$

$$\Delta E_2=E_{\rm tot}(n_d^{\uparrow}-1,n_d^{\downarrow})-E_{\rm tot}(n_d^{\uparrow}-1,n_d^{\downarrow}-1)\,. \tag{16}$$

The quantities $\Delta E_1$ and $\Delta E_2$ can be easily evaluated through transition-state procedures. They are $-0.739$ and $-1.14$ Ry. Thus, our result for Hubbard parameter is

$$U_{dd}=0.401\ \text{Ry}=5.45\ \text{eV}\,.$$

This value is in good agreement with the estimates of 5–6 eV from synchrotron-radiation photoemission studies by Takahasi *et al.*[20] and Shen *et al.*[21] This value is not large compared to the bandwidth (7–11 eV), but it is large enough so that electron correlations should be important. A fully localized picture for the Cu $d$ electrons, however, is unlikely to be appropriate.

By performing similar transition-state calculations on a single-particle state inside peak $F$ of Fig. 2, we find $E_{\rm tot}(n_p^{\uparrow},n_p^{\downarrow})-E_{\rm tot}(n_p^{\uparrow}-1,n_p^{\downarrow})=-0.533$ Ry and $E_{\rm tot}(n_p^{\uparrow}-1,n_p^{\downarrow})-E_{\rm tot}(n_p^{\uparrow}-1,n_p^{\downarrow}-1)=-0.885$ Ry. Thus, one can deduce an on-site $p$-$p$ interaction energy:

$$U_{pp}=4.79\ \text{eV}\,.$$

A Mulliken population analysis indicates this single-particle state has over 85% O $p$ nature, and its charge density is distributed mainly around one of the edge O(1) atoms. An alternative calculation of $U_{pp}$ as the difference between the ionization energy and the electron affinity gives a result of 5.2 eV for $U_{pp}$. Here, the single-particle state used for electronic affinity calculation has about 57% O$p$ character and its charge density is distributed among two-edge O(1) atoms and O(4) atoms rather evenly.

From high-energy spectroscopy experiments, Wendin[42] has deduced $U_{pp}\approx 4$ eV and $U_{dd}\approx 6$ eV, which are also in reasonable agreement with the present estimation.

Additional transition-state calculations have been performed to determine the ionization energies of some core levels. We find for the oxygen $1s$ state 39.2 Ry, for the Cu $2p$ state 69.0 Ry, and for the Cu $3p$ 5.70 Ry. These may be compared with the results of Ref. 11 (obtained from graphical data which are referenced to the Fermi level) of 38.9, 69.0, and 5.42 Ry. Presumably, these values need to be corrected by 0.2–0.3 Ry to allow for the difference between the Fermi level and the vacuum. The results for O($1s$) depend on the oxygen site chosen by only about 0.1 Ry.

## IV. SUMMARY

The electronic structure of $Ba_4Cu_2O_7$ clusters in four different charge states has been studied via an all-electron, spin-polarized, local-density functional approach. We did not find any magnetic moment on the Cu atoms. The

charge distribution in the Cu-O chain shows highly covalent bonding. The valence-band structure agrees very well with several band calculations. We find Cu $d$ states are very strongly hybridized with O $p$ states, while near the Fermi level, O $p$ states dominate.

Transition-state calculations of photoemission energies gave results in rather good agreement with experiment which indicates, contrary to some opinions, that density functional calculations can be reasonably successful in this system. Specifically, we were able to explain the shift of calculated valence-band structure near $E_F$ relative to the photoemission data. Electronic relaxation is found to be very important here. We also reported charge-transfer transition energy from Cu $d$ to O $p$ in the range of 4–5 eV, while the transition energy between O $p$ and Ba $s$ is about 6.7 eV.

A rather important conclusion from the present work is that the repulsive energy of electrons with opposite spin in copper orbitals is 5.5 and 4.8 eV for the oxygen $p$ orbitals. Together with the large relaxation effects observed, the fact that the Hubbard parameter is in the range of 50–80% of the valence bandwidth indicates moderately strong correlations between Cu $d$ electrons. We believe correlations between Cu $d$ electrons and strong hybridization between Cu $d$ and O $p$ must be very important in the mechanism of high-$T_c$ superconductivity. Single-particle local-density function calculations are not appropriate for further study of these correlation effects. However, the present results may be useful in estimating the parameters of many-body theories of the superconducting interaction.

## ACKNOWLEDGMENT

This research was supported by the U.S. Army Research Office under Contract No. DAAG29-85-K-0036.

[1]D. W. Murphy, S. A. Sunshine, P. K. Gallagher, H. M. O'Bryan, R. J. Cava, B. Batlogg, R. B. van Dover, L. F. Schneemeyer, and S. M. Zahurak, in *Chemistry of High-Temperature Superconductors,* edited by D. L. Nelson, M. S. Whittingham, and T. F. George (American Chemical Society, Washington, DC, 1987), p. 181.

[2]L. F. Mattheiss and D. R. Hamann, Solid State Commun. **63**, 395 (1987).

[3]S. Massida, J. Yu, A. J. Freeman, and D. D. Koelling, Phys. Lett. A **122**, 198 (1987).

[4]H. Krakauer and W. E. Pickett, in *Novel Superconductivity,* edited by S. A. Wolf and V. Z. Kresin (Plenum, New York, 1987), p. 501.

[5]W. Y. Ching, Y. Xu, G. L. Zhao, K. W. Wong, and F. Zandiehnadem, Phys. Rev. Lett. **59**, 1333 (1987).

[6]W. Temmerman, Z. Szotek, P. J. Durham, G. M. Stocks, and P. A. Sterne, J. Phys. Lett. F (to be published).

[7]F. Herman, R. V. Kasowski, and W. Y. Hsu, Phys. Rev. B **36**, 6904 (1987).

[8]D. W. Bullett and W. G. Dawson, J. Phys. C **20**, L853 (1987).

[9]J. Callaway and N. H. March, in *Solid State Physics,* edited by H. Ehrenreich, F. Seitz, and D. Turnbull (Academic, New York, 1984), Vol. 38, p. 135.

[10]S. Horn, J. Cai, S. A. Shaheen, Y. Jeon, M. Croff, C. L. Chang, and M. L. den Boer, Phys. Rev. B **36**, 3895 (1987).

[11]J. A. Yarmoff, D. R. Clarke, W. Drube, U. O. Karlsson, A. Taleb-Ibrahimi, and F. J. Himpsel, Phys. Rev. B **36**, 3967 (1987).

[12]Y. Jeon, F. Lu, H. Jhans, S. A. Shaheen, G. Liang, M. Croft, P. H. Ansari, K. V. Ramanujachary, E. A. Hayri, S. M. Fine, S. Li, H. Feng, M. Greenblatt, L. H. Greene, and J. M. Tarascon, Phys. Rev. B **36**, 3891 (1987).

[13]F. Zuo, B. R. Patton, D. L. Cox, S. I. Lee, Y. Song, J. P. Goldben, X. D. Chen, S. Y. Lee, Y. Cao, Y. Lu, J. R. Gaines, J. C. Garland, and A. J. Epstein, Phys. Rev. B **36**, 3603 (1987).

[14]I. Furo, A. Jánossy, L. Mihály, P. Bánki, I. Pocsik, I. Bakonyi, I. Heinmaa, E. Joon, and E. Lippmaa, Phys. Rev. B **36**, 5690 (1987).

[15]F. Mehran, S. E. Barnes, T. R. McGuire, W. J. Gallagher, R. L. Sandstrom, T. R. Dinger, and D. A. Chance, Phys. Rev. B **36**, 740 (1987).

[16]G. J. Bowden, P. R. Elliston, K. T. Wan, S. X. Dou, K. E. Easterling, A. Bourdillion, C. C. Sorrell, B. A. Cornell, and F. Separovic, J. Phys. C **20**, L545 (1987).

[17]M. A. Beno, L. Soderholm, D. W. Capone II, D. G. Hinks, J. D. Jorgenson, I. K. Shuller, C. Segre, and J. D. Grace, Appl. Phys. Lett. **51**, 57 (1987).

[18]P. D. Johnson, S. L. Qiu, L. Jiang, M. W. Ruckman, M. Strongin, S. L. Hulbert, R. F. Garrett, B. Sinkovic, N. V. Smith, R. J. Cava, C. S. Tee, D. Nichols, E. Kaczanowicz, R. E. Salomon, and J. E. Crow, Phys. Rev. B **35**, 8811 (1987).

[19]R. L. Kurtz, R. L. Stockbauer, D. Mueller, A. Shih, L. E. Toth, M. Dsofsky, and S. A. Wolf, Phys. Rev. B **35**, 8818 (1987).

[20]T. Takahashi, F. Maeda, H. Arai, H. Katayama-Yoshida, Y. Okabe, T. Suzuki, S. Hoysoya, A. Fujimori, T. Shidara, T. Koide, T. Miyahara, M. Onoda, S. Shamoto, and M. Sato, Phys. Rev. B **36**, 5686 (1987).

[21]Z. Shen, J. W. Allen, J. J. Yeh, J. S. Kang, W. Ellis, W. Spicer, I. Lindau, M. B. Maple, Y. D. Dalichaouch, M. S. Torikachvili, and J. Z. Sun (unpublished).

[22]J. Redinger, A. J. Freeman, J. Yu, and S. Massida (unpublished).

[23]H. Chen, J. Callaway, and P. K. Misra, Phys. Rev. B **36**, 8863 (1987).

[24]A. K. Rajagopal, S. P. Singhal, and J. Kimball (unpublished), as quoted by A. K. Rajogopal, in *Advances in Chemical Physics,* edited by G. I. Prigogine and S. A. Rice (Wiley, New York, 1979), Vol. 41, p. 59.

[25]Cu: A. J. H. Wachters, J. Chem. Phys. **57**, 1033 (1971); O: F. B. van Duijneveldt, IBM Research Report No. RJ945, 1971 (unpublished). Ba: S. Huzinaga, in *Gaussian Basis Sets for Molecular Calculations* (Elsevier, Amsterdam, 1984), p. 303.

[26]D. Bagayoko, Int. J. Quant. Chem. Symp. **17**, 527 (1983).

[27]H. Sambe and R. H. Felton, J. Chem. Phys. **62**, 1122 (1975).

[28]J. W. Mintmire and B. W. Dunlap, Phys. Rev. A **25**, 88 (1983).

[29]K. Lee, J. Callaway, and S. Dhar, Phys. Rev. B **30**, 1724 (1984).

[30]K. Lee, Ph.D. thesis, Louisiana State University, 1984 (unpublished) (available from University Microfilms, Ann Arbor, MI).

[31]C. B. Haselgrove, Math. Comput. **15**, 323 (1961).

[32]D. E. Ellis, Int. J. Quant. Chem. Symp. **2**, 35 (1968).

[33]D. E. Ellis and G. S. Painter, Phys. Rev. B **2**, 2887 (1970).

[34]A mapping $\{r\} \rightarrow \{\xi\}$ is used here: $r = r_0 - a^{-1}\ln[e^{a(1-\xi)/A} - 1]$ with $A = a/\ln(1+e^{ar_0})$. The points $\{r\}$ will follow the distribution of Eq. (13) if the values of $\{\xi\}$ are evenly distributed between 0 and 1.

[35]S. Y. Shashkin and W. A. Goddard, Phys. Rev. B **33**, 1353 (1986).

[36]N. E. Brener and J. Callaway, Phys. Rev. B **35**, 4001 (1987).

[37]P. Blaha and J. Callaway, Phys. Rev. B **33**, 1706 (1986).

[38]D. Vaknin, S. K. Sinka, D. E. Moncton, D. C. Johnston, J. M. Newsam, C. R. Safinya, and H. E. King, Jr., Phys. Rev. Lett. **58**, 2802 (1987).

[39]J. M. Tranquada, D. E. Cox, W. Kunnmann, H. Moudden, G. Shirane, M. Suenaga, P. Zolliker, D. Vaknin, S. K. Sinha, M. S. Alvarez, A. J. Jacobson, and D. C. Johnston, Phys. Rev. Lett. **60**, 156 (1988).

[40]Y. Guo, J. M. Langlois, and W. A. Goddard III, Science **239**, 896 (1988).

[41]For example, P. W. Anderson, Science **325**, 1196 (1987); V. J. Emery, Phys. Rev. Lett. **58**, 2794 (1987).

[42]G. Wendin, J. Phys. (Paris) (to be published).